Use of 2-Aminopurine Fluorescence To Examine Conformational Changes during Nucleotide Incorporation by DNA Polymerase I (Klenow Fragment)†

Vandana Purohit, Nigel D. F. Grindley, and Catherine M. Joyce*

Department of Molecular Biophysics and Biochemistry, Yale University, New Haven, Connecticut 06520

Received January 21, 2003; Revised Manuscript Received July 3, 2003

ABSTRACT: We have investigated conformational transitions in the Klenow fragment polymerase reaction by stopped-flow fluorescence using DNA substrates containing the fluorescent reporter 2-aminopurine (2-AP) on the template strand, either at the templating position opposite the incoming nucleotide (designated the 0 position) or 5′ to the templating base (the +1 position). By using both deoxy- and dideoxy-terminated primers, we were able to distinguish steps that accompany ternary complex formation from those that occur during nucleotide incorporation. The fluorescence changes revealed two extremely rapid steps that occur early in the pathway for correct nucleotide incorporation. The first, detectable with the 2-AP reporter at the 0 position, occurs within the first few milliseconds and is associated with dNTP binding. This is followed by a rapid step involving relative movement of the +1 base, detectable when the 2-AP reporter is at the +1 position. Finally, when the primer had a 3′-OH, a fluorescence decrease with a rate equal to the rate of nucleotide incorporation was observed with both 0 and +1 position reporters. When the primer was dideoxy-terminated, the only change observed at the rate expected for nucleotide incorporation had a very small amplitude, suggesting that the rate-limiting conformational change does not produce a large fluorescence change, and is therefore unlikely to involve a significant change in the environment of the fluorophore. Fluorescence changes observed during misincorporation were substantially different from those observed during correct nucleotide incorporation, implying that the conformations adopted during correct and incorrect nucleotide incorporation are distinct.

The Klenow fragment (KF)[1] of DNA polymerase I from *Escherichia coli* contains the DNA polymerase and 3′−5′ proofreading exonuclease activities of the parent molecule and has long served as an excellent model system for studying the molecular mechanism of template-directed DNA synthesis. The early structural studies of Klenow fragment (*1*) gave the first view of a polymerase domain whose essential structural features are conserved throughout the polymerase superfamily (*2*). Similarly, the extensive kinetic studies that established the minimal kinetic scheme for KF and the mutational experiments that identified key active site residues (reviewed in refs *3* and *4*) have close parallels in other DNA polymerase systems, both homologous and nonhomologous.

Typical of other polymerase domain structures, the polymerase domain of KF resembles a partially open right hand with three subdomains, designated "fingers", "palm", and "thumb". The palm subdomain contains a well-conserved structural motif, the "polymerase fold", which serves as the scaffold for important catalytic residues, including the aspartate side chains which bind the two divalent metal ions required for catalysis of phosphoryl transfer (*4*, *5*). The fingers and thumb subdomains form the sides of the polymerase cleft. The thumb binds the template-primer duplex upstream of the site of nucleotide addition, while the fingers subdomain binds the single-stranded template beyond the site of nucleotide addition and also contributes residues that form the binding site for the nascent base pair. No cocrystal structures of KF have been obtained with substrates at the polymerase active site; however, structures of three other Pol I family polymerases with DNA in the polymerase active site have been solved. These are the Klenow fragment-like portions of *Taq* DNA polymerase (Klentaq) and *Bacillus stearothermophilus* DNA polymerase (*Bst* pol), and the DNA polymerase of bacteriophage T7 (T7 DNA pol). These polymerases have a high degree of sequence and structural homology to KF, such that virtually all of the active site residues are conserved and the structures can serve as representative models for KF.

The cocrystal structures of Pol I family polymerases include both binary (pol·DNA) and ternary (pol·DNA·dNTP) complexes. The binary complexes of Klentaq and *Bst* pol resemble the uncomplexed KF structure in terms of the general architecture of the subdomains (*6*, *7*). The primer-template duplex is bound in a shallow cleft between the thumb and the 3′−5′ exonuclease domain, with the fingers subdomain serving to anchor both the primer and template strands in the polymerase active site. The Klentaq, *Bst* pol,

† This work was supported by Grant GM-28550 from the National Institutes of Health.

* To whom correspondence should be addressed. Phone: (203) 432-8992. Fax: (203) 432-3104. E-mail: catherine.joyce@yale.edu.

[1] Abbreviations: KF, Klenow fragment (large fragment of *Escherichia coli* DNA polymerase I); Klentaq, large fragment of *Thermus aquaticus* DNA polymerase I; *Bst* pol, large fragment of *Bacillus stearothermophilus* DNA polymerase I; T7 DNA pol, DNA polymerase of bacteriophage T7; pol β, DNA polymerase β; dNTP, deoxynucleoside triphosphate; 2-AP, 2-aminopurine; $KMnO_4$, potassium permanganate.

10.1021/bi0341206 CCC: $25.00
Published on Web 08/09/2003

Scheme 1

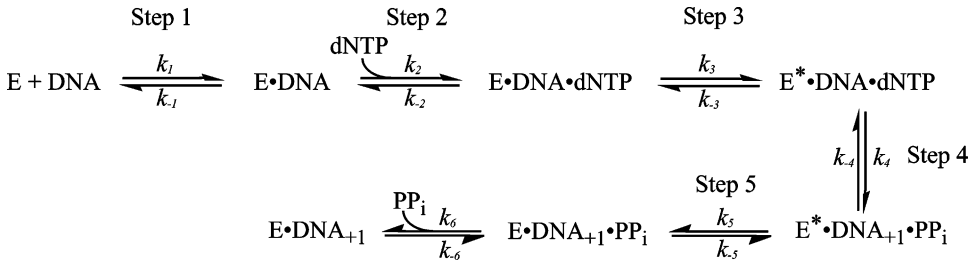

and T7 DNA pol ternary complexes (*6*, *8*, *9*) reveal a striking rotation of the fingers subdomain toward the active site when compared to the binary complex structures. This movement of the fingers subdomain forms a more closed active site, with a snug binding pocket for the nascent base pair. The O helix, which spans the fingers subdomain, forms one wall of the binding pocket and contributes several highly conserved residues which contact the sugar and phosphates of the incoming nucleotide. Comparison of the binary and ternary complex structures therefore suggests that, following dNTP binding, there is a conformational change of the polymerase from an "open" to a "closed" form. Analogous subdomain rotations have been documented in structurally homologous polymerases from other families, namely RB69 DNA polymerase and HIV-1 reverse transcriptase (*10*, *11*), and also in mammalian DNA polymerase β (pol β), which is a member of the nucleotidyl transferase family (*12*, *13*).

Extensive studies by Benkovic and co-workers have established a minimal kinetic mechanism for correct nucleotide incorporation by KF (Scheme 1) (*3*, *14*, *15*). The first step involves binding of primer-template DNA to KF; this is followed by binding of dNTP to the E·DNA complex (step 2). In KF, the K_d for binding an incorrect nucleotide is typically 10−100-fold higher than for correct nucleotide binding (*16*−*18*), so that step 2 is expected to contribute to fidelity, though to a lesser extent than in some replicative polymerases, such as T7 DNA pol, where the difference in K_d for correct and incorrect nucleotides is larger (*19*). Following dNTP binding, step 3 is a slow noncovalent transformation that has been described as "a conformational change of the ternary complex to a form poised for nucleophilic displacement" (*20*). Step 4 is phosphoryl transfer, which is followed by a second noncovalent transformation, pyrophosphate release, and translocation or dissociation. In KF, there is convincing evidence for the existence of the noncovalent "conformational change" steps from pulse−quench and pulse−chase experiments (*15*); however, in other systems, the evidence for analogous steps is weaker in that it relies primarily on elemental effect measurements whose interpretation can be ambiguous (discussed in refs *21*−*24*). Step 4 (phosphoryl transfer) provides a major contribution to polymerase fidelity; it is extremely rapid when incorporating a correctly paired dNTP but becomes the rate-limiting step in misincorporation (*14*, *16*). The subsequent conformational change (step 5) is also slowed when an incorrect dNTP is added, and this too contributes to fidelity by providing an opportunity for editing (*14*, *16*).

A popular hypothesis is that the closing of the fingers inferred from polymerase crystal structures corresponds to the rate-limiting conformational change that precedes phosphoryl transfer in the kinetic scheme described above (*6*, *25*). However, recent evidence, especially in the pol β system, raises doubts about this conclusion and suggests instead that the closing of the polymerase domain occurs at a rapid rate and the rate-limiting step may involve smaller adjustments that take place within the closed complex (*26*−*29*).

In this study we have used fluorescence to examine noncovalent steps that occur along the polymerase reaction pathway of KF. Conventional rapid-quench techniques using radiolabeled primers have been invaluable in studies of the kinetics of nucleotide incorporation, but because they rely on measuring the formation of an extended product, they can only report on noncovalent processes if those steps happen to be rate-limiting. Stopped-flow fluorescence measurements, on the other hand, allow the study of noncovalent changes on a fast time scale. To probe conformational changes of the KF·DNA complex, we have used 2-aminopurine (2-AP), a fluorescent nucleotide analogue that base pairs with thymine without distortion of the helix (*30*). 2-AP serves as a useful probe for conformational changes because its fluorescence is extremely sensitive to its environment, being quenched primarily by intrastrand base stacking interactions with neighboring bases (*31*). Recent studies using 2-AP fluorescence have been informative in several polymerase systems (*26*, *29*, *32*−*34*), including a preliminary study of KF (*35*).

EXPERIMENTAL PROCEDURES

Materials. Deoxynucleoside triphosphates and [γ-^{32}P]ATP were purchased from Amersham Pharmacia Biotech. DNA oligonucleotides (Figure 1) were synthesized by the Keck Biotechnology Resource Laboratory at Yale Medical School and purified by denaturing polyacrylamide gel electrophoresis. DNA templates and primers were annealed in 50 mM Tris-HCl (pH 7.5) and 10 mM $MgCl_2$ (or 2.5 mM $MnCl_2$ when Mn^{2+} was used instead of Mg^{2+}) by heating to 65 °C and slow cooling to room temperature over several hours.

Enzyme Purification. Derivatives of Klenow fragment, containing the D424A mutation that eliminates exonuclease activity (*36*), were purified to homogeneity by our standard procedure (*37*) modified as described (*38*). The D424A,-F771A Klenow fragment mutant was kindly provided by Robert M. Turner, Jr. (*38*).

Steady-State Fluorescence Emission Spectra. Emission spectra of 2-AP-containing duplexes were obtained with a Photon Technology International scanning spectrofluorometer. Samples were excited at 310 nm, and fluorescence spectra were collected from 330 to 460 nm. DNA duplexes (10 μM 2-AP-containing template, 20 μM primer) were annealed as described above. Solutions for fluorescence measurements contained 1 μM duplex DNA and, as ap-

propriate, 4 μM KF and dNTP (as specified in the figures) in 50 mM Tris-HCl (pH 7.5) and 10 mM $MgCl_2$. Enzyme titrations were performed to determine the enzyme:DNA ratio necessary to produce the maximum change in the fluorescence signal from the 2-AP-containing DNA. Spectra were corrected by subtraction of emission data from identical control solutions lacking the 2-AP-containing duplex DNA.

Rapid Chemical Quench Experiments. Single-turnover measurements of nucleotide incorporation were carried out at room temperature (21 °C) in a rapid quench-flow instrument (KinTek Corp., Model RQF-3) as described previously (*39*). The final concentrations in a typical reaction mixture were 20 nM duplex, 1 μM KF, 50 mM Tris-HCl (pH 7.5), 10 mM $MgCl_2$, and varying concentrations of dNTP.

Stopped-Flow Fluorescence Experiments. Stopped-flow experiments were performed at 21 °C using an Applied Photophysics SX.18 MV spectrofluorometer with a Hg−Xe lamp. A solution of 2-AP-containing duplex DNA and KF was rapidly mixed (dead time ≈ 2 ms) with a dNTP solution, giving final concentrations of 200 nM 2-AP-containing template, 400 nM primer, and 800 nM KF. Both solutions contained 50 mM Tris-HCl (pH 7.5) and 10 mM $MgCl_2$, unless otherwise specified. The dNTP concentrations were varied as indicated in individual figures. The excitation wavelength was 313 nm, and the progress of the reaction was monitored by measuring fluorescence emission using a 345 nm cut-on filter. Data were collected for at least 10 s, and longer for slow reactions. Three to five traces were averaged for each experiment. Curves were fitted over at least 10 half-lives, using Pro-K for Windows (Applied Photophysics), to calculate the rate of change in fluorescence. The data were analyzed as either a single-step (A → B) or a two-step (A → B, B → C) process, and the quality of the fit was evaluated on the basis of the residuals. See Figures S1−S3 (Supporting Information) for examples of the curve fitting.

Use of $KMnO_4$ To Probe Thymine Reactivity. The template 5′-CTAGACACTTGGTCGTCGTGACGGCTGCGA-3′, 5′-labeled with ^{32}P, was annealed to a 4-fold molar excess of the dideoxy-terminated primer 5′-TCGCAGCCGTCAC^{dd}-3′. KF was added to the DNA duplex, giving 40 nM duplex and 1 μM KF in a total volume of 25 μL of 50 mM Tris-HCl (pH 7.5) and 10 mM $MgCl_2$. In some samples, a dNTP was present in order to form the ternary complex. The complexes were treated with 3 μL of freshly prepared 25 mM $KMnO_4$ for 30 s at 21 °C, and the reaction was terminated by addition of 3 μL of β-mercaptoethanol. The DNA was precipitated and treated with piperidine following the procedure employed in Maxam−Gilbert sequencing (*40*). Cleavage products were analyzed on a 12% polyacrylamide−urea gel and quantitated by phosphorimager analysis. To correct for loading differences between lanes, the intensity of the band that resulted from cleavage at the +1 position was normalized to one of the bands produced by cleavage of the thymines at the +7 or +8 positions. The reactivity of the +7 and +8 positions was shown to be unaffected by the addition of KF or dNTP, and calculations using either band as a reference gave the same results.

RESULTS

DNA Substrates. To investigate conformational changes of the KF·DNA complex during nucleotide incorporation, we used DNA substrates having a single fluorescent base (2-AP) on the template strand, annealed to both normal (2′-deoxy) and 2′,3′-dideoxy-terminated primers (Figure 1). From structural data, we reasoned that the conformational changes that take place during the polymerase reaction should have substantial effects on the environment of the templating base that will pair with the incoming nucleotide (designated the 0 position) and its 5′ neighbor (designated the +1 position), and we therefore chose to study DNA substrates with 2-AP at these two positions. In our numbering system (Figure 1A), the primer terminal base pair would be described as the −1 position, and the numbering does not change on going from binary to ternary complexes. Thus, the 0 position is not base paired in the KF·DNA binary complex but is base paired to the incoming nucleotide in the KF·DNA·dNTP ternary complex. We used two different positions for the 2-AP fluorescent reporter in order to increase the chances of observing conformational changes, since some may be observable only with a particular location of the reporter. Additionally, an important part of the experimental design was the use of both deoxy- and dideoxy-terminated primers. The use of normal 2′-deoxy-terminated primers allows nucleotide incorporation to take place. With a 2′,3′-dideoxy-terminated primer, phosphoryl transfer cannot take place, and we can therefore focus on steps leading to the formation of a ternary complex, but not including phosphoryl transfer. For all of the substrates, we used both static measurements, to determine the effect of various reaction components on the 2-AP fluorescence emission spectrum, and stopped-flow fluorescence in order to measure the rates of the observed fluorescence change(s).

A

5′-TCGCAGCCGTCAC-3′
3′-AGCGTCGGCAGTGXAACCCC-5′
-1 0 +1 +2

B

Primers
dP 5′-TCGCAGCCGTCAC-3′
ddP 5′-TCGCAGCCGTCAC^{dd}-3′

Templates
0 position
0T1 3′-AGCGTCGGCAGTGXAACCCC-5′
0T2 3′-AGCGTCGGCAGTGXCCCAAA-5′

+1 position
+1T1 3′-AGCGTCGGCAGTGCXCCAAA-5′
+1T2 3′-AGCGTCGGCAGTGGXCCAAA-5′
+1T3 3′-AGCGTCGGCAGTGTXCCAAA-5′
+1T4 3′-AGCGTCGGCAGTGCXYCAAA-5′
+1T5 3′-AGCGTCGGCAGTGGXYCAAA-5′

FIGURE 1: (A) Nomenclature used to identify positions on the template strand. In this case, 2-AP (indicated by an X) is in the 0 position. (B) Sequence of oligonucleotides used in the fluorescence studies. The template base at the 0 position is underlined, 2-AP is indicated by an X, a tetrahydrofuran abasic site is indicated by a Y, and a 2′,3′-dideoxy-C is indicated by C^{dd}.

Throughout these experiments exonuclease-deficient KF (D424A) was used in order to avoid complications due to the proofreading exonuclease activity. For simplicity, KF mutants are described by the genotype of the polymerase domain, so that the D424A mutant is referred to as wild type and the mutant described as F771A corresponds to the double mutant D424A,F771A.

Addition of the Correct Nucleotide: 2-AP at the 0 Position. Figure 2A shows the fluorescence emission spectrum of a template DNA containing 2-AP at the 0 position annealed to a normal (deoxy-terminated) primer. Addition of KF to

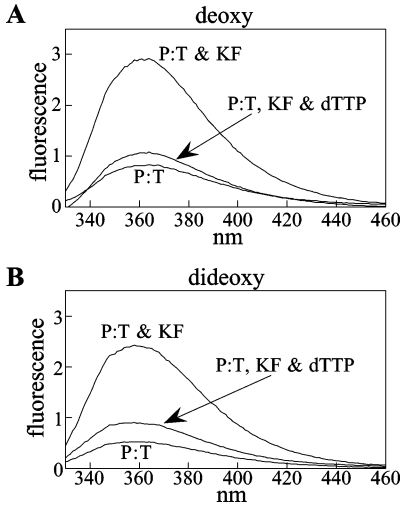

FIGURE 2: Fluorescence emission spectra of DNA duplexes (Figure 1B) containing 2-AP at the 0 position on the template strand. Spectra were recorded of duplex DNA alone, in a binary complex with KF, and after addition of dTTP. (A) dP·0T1 duplex. dTTP was added at 10 μM. (B) ddP·0T1 duplex. dTTP was added at 400 μM, based on titrations showing that this concentration is sufficient to produce the maximum fluorescence change for the E·DNA·dNTP ternary complex. The emission spectrum labeled "P:T, KF, and dTTP" therefore represents a ternary complex.

form a binary complex caused a 3-fold increase in fluorescence. Subsequent addition of dTTP, which can be incorporated by forming a Watson−Crick base pair opposite 2-AP, resulted in a decrease in fluorescence. When the primer was dideoxy-terminated (Figure 2B), similar changes were observed except that the decrease in fluorescence upon addition of dTTP was about half of that observed when incorporation of dTTP could take place.

These same substrates were studied using the stopped-flow instrument to monitor the changes in fluorescence as a function of time (Figure 3A,B). When a solution containing a binary complex of KF and primer-template DNA (either deoxy or dideoxy terminated) was mixed with a solution containing dTTP, a substantial decrease in fluorescence took place within the dead time of the instrument (approximately 2 ms, indicated in Figure 3A,B as a dotted line). With a deoxy-terminated primer, the initial rapid decrease was followed by another large fluorescence decrease, corresponding to a single exponential decay whose rate was similar to the rate of nucleotide incorporation as determined by rapid-quench experiments with the same substrates (Figure 3C). Analysis of the rate of this second process, from four independent experiments, gave a k_{pol} of 40 s^{-1} and K_d(dNTP) of 71 μM for incorporation of dTTP opposite 2-AP (Table 1); compare k_{pol} of 87 s^{-1} and K_d(dNTP) of 20 μM for incorporation of dTTP opposite A in a different oligonucleotide sequence (*39*). The second fluorescence decay was absent when using a dideoxy-terminated primer (Figure 3B), consistent with the emission spectral data. We carefully analyzed the fluorescence decrease that took place within the instrument dead time by comparing measurements, at a series of dTTP concentrations, that were carried out successively using the same KF·DNA solution and keeping the instrument settings constant. With both DNA substrates, the initial fluorescence signal (*Y*-axis intercept) from the stopped-flow experiment was lower after addition of dTTP than when dTTP was omitted and the KF·DNA solution was mixed only with reaction buffer (Figure 3A,B). In experiments with the deoxy-terminated primer, the *Y*-axis intercept showed the same dependence on dTTP concentration as did the rate of nucleotide incorporation (Figure 3D); with the dideoxy-terminated primer, the dTTP dependence of the *Y*-axis intercept suggested ≈3-fold lower affinity for dTTP (Table 1). Similar baseline movement and fluorescence transients were observed when a different substrate with 2-AP at the 0 position was used (template 0T2; data not shown). To ensure that the initial fluorescence changes were not caused by collisional quenching of 2-AP following addition of dTTP, measurements were repeated in the absence of added Mg^{2+} and in 1 mM EDTA. In this situation, addition of up to 500 μM dTTP caused no decrease in fluorescence (data not shown).

In addition to the major features of the stopped-flow data described in the preceding paragraph, other more subtle fluorescence changes were apparent on close examination of Figure 3A,B. With both deoxy- and dideoxy-terminated primers, a rapid but small fluorescence decrease was observed immediately after the instrument dead time of ≈2 ms; this was probably the tail end of the process that occurred within the instrument dead time. With the deoxy-terminated primer, the initial decrease was followed by a slight increase and, finally, the large fluorescence decay (rate = k_{pol}) described above. Because of the small amplitudes and rapid rates of these early processes, they were impossible to quantitate accurately and were not analyzed further. Following the initial rapid decrease, the fluorescence signal from the dideoxy-terminated substrate consistently gave a very low amplitude decay that was observable over 100−200 ms (Figure 3B). Over the same interval, the fluorescence of a control sample without dTTP remained constant, indicating that photobleaching was unlikely to be the cause of the fluorescence decrease. Attempts to fit the data obtained at high dTTP concentrations (≥100 μM) gave a rate of ≈20 s^{-1} for the low amplitude decay. Because of the difficulty in analyzing these signals, however, the rate estimates should be interpreted extremely cautiously.

To explore whether the dideoxy-terminated primer may influence metal binding due to the loss of a ligand at the metal A site, we manipulated the metal ion cofactor in ways that should compensate for lower binding affinity. Increasing the Mg^{2+} concentration from 10 to 50 mM had no effect on the observed fluorescence changes (data not shown). We also examined the fluorescence changes that occur when the tighter binding Mn^{2+} (*41*) replaces Mg^{2+} in the polymerase reaction. Figure 3E shows a sample of the data obtained in the presence of 2.5 mM Mn^{2+}; the same reactions carried out with 10 mM Mg^{2+} are shown for comparison in Figure 3F. With a deoxy-terminated primer and 2-AP at the 0 position, the reaction in the presence of Mn^{2+} (dP, Figure 3E) was very similar to that in the presence of Mg^{2+} (dP, Figure 3F): rapid initial fluorescence changes were followed by a slow fluorescence decay whose rate (≈18 s^{-1}) was similar to the rate of nucleotide incorporation (data not shown). With the dideoxy-terminated primer, the use of Mn^{2+} did not result in any substantial fluorescence changes at a rate likely to correspond to step 3; comparison of the "ddP" traces in panels E and F of Figure 3 shows that the only changes detected over the relevant time scale were the low-amplitude changes described in the previous paragraph. The

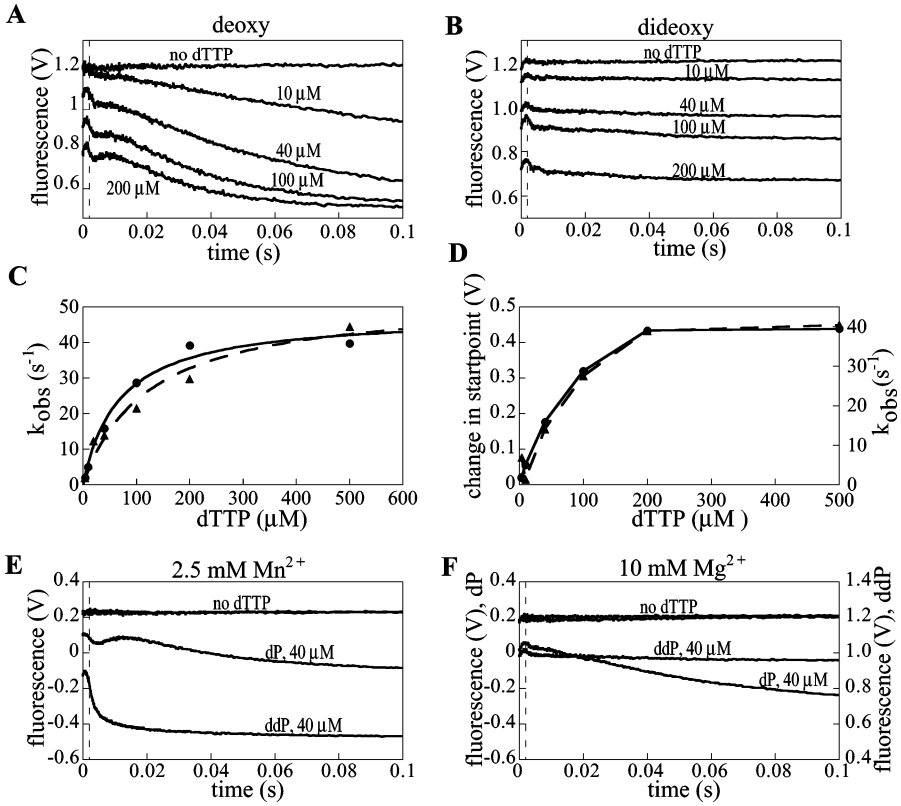

FIGURE 3: Stopped-flow kinetics using DNA duplexes containing 2-AP at the 0 position on the template strand. Measurements and data analysis were performed as described under Experimental Procedures. The traces in panels A, B, E, and F indicate fluorescence changes observed after addition of dTTP at the specified concentrations. The dotted line at 2 ms indicates the instrument dead time. For panels A, B, and F, the buffer used contained 10 mM $MgCl_2$; for panel E, 2.5 mM $MnCl_2$ was used instead of $MgCl_2$. (A) dP·0T1 duplex. Following the initial rapid changes, the major fluorescence decay was fit to a single exponential with rates of 5, 16, 29, and 38 s^{-1} for 10, 40, 100, and 200 μM dTTP, respectively. See Figure S1 in Supporting Information for an example of the curve fitting. (B) ddP·0T1 duplex. (C) Pre-steady-state kinetics of dTTP incorporation into the dP·0T1 substrate. (▲) Rates of dTTP incorporation, as a function of dTTP concentration, obtained from rapid-quench experiments as described under Experimental Procedures; fitting of these data to a hyperbolic equation gave $k_{pol} = 53 \pm 6$ s^{-1} and K_d(dTTP) = 120 μM. (●) Rates of fluorescence decay, as a function of dTTP concentration, obtained from the stopped-flow experiment illustrated in panel A; fitting of these data to a hyperbolic equation gave $k_{pol} = 48 \pm 3$ s^{-1} and K_d(dTTP) = 70 μM. (D) Fluorescence changes observed in stopped-flow experiments with the dP·0T1 substrate. The data are taken from the experiment illustrated in panel A. The change in initial signal voltage (*Y*-axis intercept) (▲) and the rate of fluorescence decay (●) are plotted as a function of dTTP concentration. (E) Fluorescence changes in the presence of 2.5 mM $MnCl_2$. The traces labeled dP and ddP correspond to fluorescence changes observed upon mixing 40 μM dTTP with binary complexes of KF with dP·0T1 and ddP·0T1, respectively. The control traces, obtained in the absence of dTTP, were essentially superimposable. For the deoxy-terminated primer (dP), the small initial fluorescence changes were not quantitated, and the rate of the major fluorescence decay was 18 s^{-1}. For the dideoxy-terminated primer (ddP), the rate of the major fluorescence decay was 340 s^{-1}. (F) Fluorescence changes in the presence of 10 mM $MgCl_2$ for reactions analogous to those shown in panel E. The traces are presented as a double *Y*-axis plot to facilitate the comparison with panel E. The rate of the major fluorescence decay for the deoxy-terminated primer (dP) was 13 s^{-1}.

Table 1: Rate Constants Determined by Stopped-Flow Fluorescence

reaction[a]	DNA duplex[b]	kinetic parameters[c]	no. of expts
2-AP·dTTP	dP·0T1 (2-AP at 0 position)	rate 1: $\geq$1000 s^{-1} [d] rate 2: k_{pol} 40 ± 7 s^{-1}, K_d 71 ± 12 μM	4
2-AP·dTTP	ddP·0T1 (2-AP at 0 position)	rate 1: $\geq$1000 s^{-1},[d] K_d 240 ± 50 μM[e] rate 2: $\approx$20 s^{-1}	3
C-dGTP	dP·+1T1 (2-AP at +1 position)	rate 1: 160−630 s^{-1} for 1−30 μM dGTP rate 2: k_{pol} 72 ± 10 s^{-1}, K_d 2.3 ± 0.8 μM	2
C-dGTP	ddP·+1T1 (2-AP at +1 position)	rate 1: 240−850 s^{-1} for 1−20 μM dGTP rate 2: $\approx$20 s^{-1}	2

[a] Template base and incoming dNTP. [b] See Figure 1 for oligonucleotide sequences. [c] Data from two or more independent experiments were averaged, where appropriate, and are reported as mean ± SD. Rates that were extremely fast (rate 1 in either reaction) or had very low amplitude (rate 2 in reactions with the dideoxy-terminated primer) could only be determined approximately. [d] Rate 1 in the reactions with 2-AP at the 0 position corresponds to the fluorescence decrease that takes place largely within the instrument dead time. The lower limit of the rate was estimated by assuming that ≥90% of the reaction had taken place within 2 ms. [e] From plotting the change in the *Y*-axis intercept (corresponding to the fluorescence decrease that occurs within the instrument dead time) against dTTP concentration (see Figure 3D).

rapid initial fluorescence decreases observed with both deoxy- and dideoxy-terminated substrates in the presence of Mn^{2+} are probably analogous to the step that produces the rapid baseline decrease in experiments conducted in the presence of Mg^{2+}, but were slightly slower. Curiously, the amplitude of the rapid initial fluorescence decrease (rate

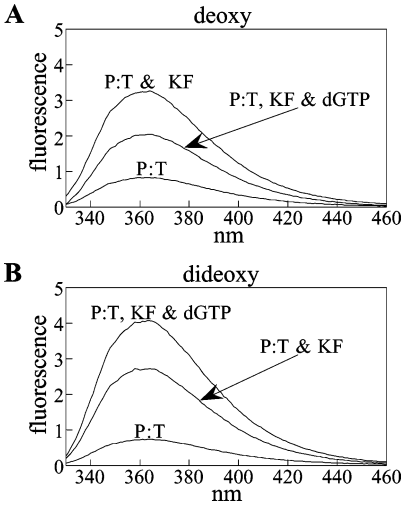

FIGURE 4: Fluorescence emission spectra of DNA duplexes (Figure 1B) containing 2-AP at the +1 position on the template strand. Spectra were recorded of duplex DNA alone, in a binary complex with KF, and after addition of 10 μM dGTP (A) dP•+1T1 duplex. (B) ddP•+1T1 duplex.

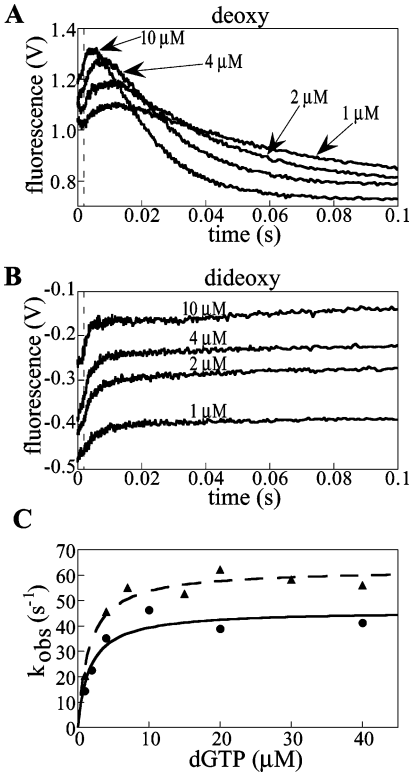

FIGURE 5: Stopped-flow kinetics using DNA duplexes containing 2-AP at the +1 position on the template strand. Measurements and data analysis were performed as described under Experimental Procedures. The traces indicate fluorescence changes observed after addition of dGTP at the specified concentrations. The dotted line at 2 ms indicates the instrument dead time. (A) dP•+1T1 duplex. The data were fit to a two-step process with the following rates: 1 μM dGTP, $r_1 = 154$ s^{-1} and $r_2 = 17$ s^{-1}; 2 μM dGTP, $r_1 = 156$ s^{-1} and $r_2 = 31$ s^{-1}; 4 μM dGTP, $r_1 = 167$ s^{-1} and $r_2 = 52$ s^{-1}; 10 μM dGTP, $r_1 = 275$ s^{-1} and $r_2 = 59$ s^{-1}. See Figure S2 in Supporting Information for an example of the curve fitting. (B) ddP•+1T1 duplex. The data were fit to a two-step process with the following rates: 1 μM dGTP, $r_1 = 242$ s^{-1} and $r_2 = 20$ s^{-1}; 2 μM dGTP, $r_1 = 389$ s^{-1} and $r_2 = 28$ s^{-1}; 4 μM dGTP, $r_1 = 411$ s^{-1} and $r_2 = 18$ s^{-1}; 10 μM dGTP, $r_1 = 589$ s^{-1} and $r_2 = 12$ s^{-1}. See Figure S3 in Supporting Information for examples of the curve fitting to a one-step or two-step process. (C) Pre-steady-state kinetics of dGTP incorporation using duplex DNA containing 2-AP at the +1 position (dP•+1T1). (●) Rates of dGTP incorporation, as a function of dGTP concentration, obtained from rapid-quench experiments as described under Experimental Procedures; fitting of these data to a hyperbolic equation gave $k_{pol} = 46 \pm 4$ s^{-1} and K_d(dGTP) = 1.7 μM. (▲) Rate 2 obtained from a stopped-flow experiment similar to the one illustrated in panel A; fitting of these data to a hyperbolic equation gave $k_{pol} = 62 \pm 3$ s^{-1} and K_d(dGTP) = 1.6 μM.

≈340 s^{-1}) seen with Mn^{2+} and a dideoxy-terminated substrate (ddP, Figure 3E) was substantially greater than that in any of the other reactions shown in Figure 3E,F. With a deoxy-terminated primer in the presence of either Mn^{2+} or Mg^{2+}, the initial rapid fluorescence decrease was immediately followed by a small fluorescence increase preceding the decrease associated with nucleotide addition to the primer terminus. These initial changes were more easily visualized in the Mn^{2+}-catalyzed reactions because of their slightly slower rates.

Addition of the Correct Nucleotide: 2-AP at the +1 Position. Binding of KF to DNA primer-template duplexes with 2-AP at the template +1 position caused a substantial (≈4-fold) increase in fluorescence (Figure 4), similar to our observations described above with 2-AP at the 0 position. With a deoxy-terminated primer and 2-AP at the +1 position, incorporation of the dNTP complementary to the templating (0 position) base produced a decrease in fluorescence. However, with the dideoxy-terminated primer, the fluorescence increased upon addition of the correct dNTP to form the ternary complex.

When dNTP additions to substrates with 2-AP at the +1 position were examined using the stopped-flow instrument, both the deoxy- and dideoxy-terminated substrates gave a rapid fluorescence increase (Figure 5A,B). In the case of the deoxy-terminated primer, the fluorescence increase was followed by a decrease whose rate corresponded to the rate of nucleotide incorporation, determined by rapid-quench experiments using the same substrates (Figure 5C). The combination of these two processes gave the overall decrease seen in the emission spectra (Figure 4A). With the dideoxy-terminated primer, the initial rapid fluorescence increase was followed by a slower increase (rate ≈20 s^{-1}) with a very low amplitude (Figure 5B), which may be related to the low-amplitude decrease detected with the 0 position 2-AP reporter. The rate of the rapid initial fluorescence increase observed with these substrates was dependent on the concentration of the correct dNTP, achieving a rate of over 500 s^{-1}. The results shown in Figures 4 and 5, and summarized in Table 1, are for incorporation of dGTP opposite a template C adjacent to the +1 position 2-AP reporter (template +1T1, Figure 1B). Similar fluorescence changes were observed for dCTP incorporation opposite G and dATP incorporation opposite T (data not shown, templates +1T2 and +1T3, respectively).

We reasoned that the changes of environment of the +1 template base that result in the observed fluorescence transients might be due to changes in stacking with its 5′ neighbor (+2 position). We therefore repeated the stopped-flow measurements with templates containing 2-AP at the +1 position and an abasic site at the +2 position (+1T4 and +1T5). The fluorescence traces obtained with these substrates (data not shown) were similar in appearance to those obtained with substrates containing a normal base at

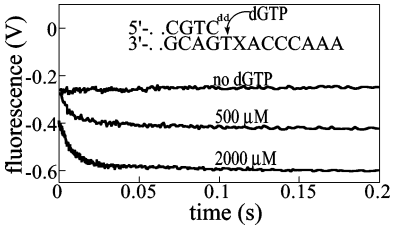

FIGURE 6: Stopped-flow kinetics for dGTP addition to a DNA duplex containing T at the 0 position and 2-AP at the +1 position (template, 5′-AAACCCAXTGACGGCTGCGA-3′, where X is 2-AP; primer, 5′-TCGCAGCCGTC^{dd}-3′). The schematic within the figure illustrates the sequence surrounding the primer terminus. Measurements and data analysis were performed as described under Experimental Procedures. The traces indicate fluorescence changes observed after addition of dGTP at the specified concentrations. The rates of fluorescence decay were 86 and 126 s^{-1} at 500 and 2000 μM dGTP, respectively.

the +2 position and gave similar reaction rates, suggesting that changes in stacking with the +2 base are not a major factor in determining the fluorescence signals from the +1 2-AP reporter.[2] We also examined the effect of the F771A mutation, which removes a side chain that is expected to stack with the +1 base. Using the +1T1 template with the dideoxy-terminated primer, the rate of the fluorescence increase was decreased about 2-fold as a result of the mutation (data not shown). In the fluorescence emission spectra of the same substrate, the F771A mutation caused an increase of ≈30% in 2-AP fluorescence for both binary and ternary complexes (data not shown), so that the ratio of ternary to binary complex emission signals was the same (≈1.5) for wild type and F771A Klenow fragment. This result suggests that F771A plays some role in quenching the fluorescence of the +1 2-AP reporter, but the interaction does not change substantially in the transition from binary to ternary complex.

Addition of Incorrect Nucleotides. We have examined the addition of incorrectly paired dNTPs with the 2-AP reporter at the opposing 0 position or at the +1 position. The observed fluorescence changes varied from mispair to mispair and, in almost all cases, were quite different from those obtained with correctly paired dNTPs. The difference in fluorescence signals between correct and mismatched pairings is illustrated very clearly by data obtained with the +1 position 2-AP reporter, where none of the mispair combinations we investigated gave the fluorescence increase (rate ≈500 s^{-1}) characteristic of a correctly paired incoming nucleotide. Figure 6 shows data for a T-dGTP mispair with 2-AP at the +1 position; we also studied all three possible mispairs opposite both template C and template G (templates +1T1 and +1T2, respectively). The results in Figure 6 are typical of our observations with all these mispairs. A decrease in fluorescence occurred within the first 100 ms; this was slower than processes observed with correct nucleotides and these templates but substantially faster than chemical incorporation of the incorrect nucleotide, observed as a very slow fluorescence decay when a deoxy-terminated primer was used (≈0.08 s^{-1} for T-dGTP). For some mispairs the observed fluorescence changes were preceded by baseline adjustments within the instrument dead time, but the magnitude and direction of these adjustments did not show a consistent pattern from mispair to mispair.

[2] Because the abasic substitution changes the fluorescence of the uncomplexed DNA substrate, it is impossible to measure the effect of the +2 abasic site on the amplitude of the fluorescence increase. Thus we cannot rule out some interaction of the +2 base with a +1 2-AP reporter.

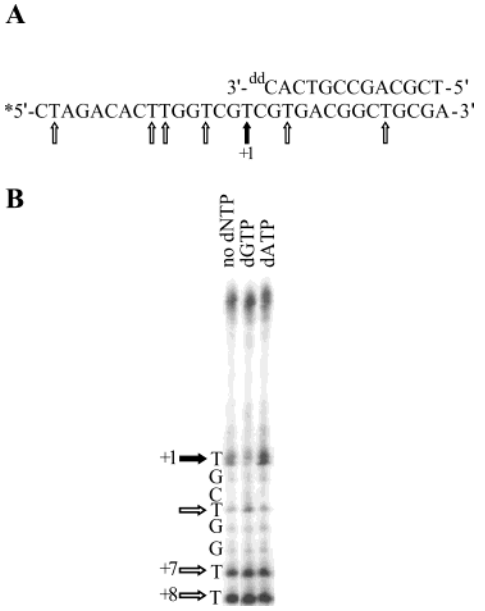

FIGURE 7: Chemical reactivity of thymine at the +1 position. (A) DNA duplex used in this experiment. The primer was dideoxy-terminated in order to allow formation of a ternary complex upon addition of dNTP. The arrows indicate the thymine residues on the template strand with the darkened arrow at the +1 position. (B) 12% polyacrylamide−urea gel showing $KMnO_4$-induced cleavage of the template strand. The reactions and quantitation were carried out as described under Experimental Procedures. The darkened arrow indicates the band that results from the cleavage of thymine at the +1 position. The intensity of the band at the +1 position was normalized to the bands resulting from cleavage of thymine at the +7 and +8 positions (indicated in the figure). The three lanes show cleavage reactions performed in the absence of dNTP, in the presence of 60 μM dGTP (forming a nascent C·dGTP base pair), and in the presence of 300 μM dATP (forming a C·dATP mispair).

Environment of the +1 Base. Chemical reactivity was used as a probe for differences in the environment of the +1 base in binary and ternary complexes. Templates containing a T at the +1 position (Figure 7A) were annealed to dideoxy-terminated primers and treated with potassium permanganate ($KMnO_4$). The reactivity of a T at the +1 position was measured in a binary complex with KF and in ternary complexes with either dGTP (correct) or dATP (incorrect) paired with the templating C (Figure 7B). Formation of the ternary complex with a correct dNTP resulted in a 20% decrease in reactivity of the +1 base relative to the binary complex. By contrast, the reactivity of the +1 base was enhanced by 45% relative to the binary complex when present in a ternary complex with an incorrect dNTP. A control experiment showed that addition of dGTP or dATP in the absence of KF had no effect on the reactivity of the +1 position.

DISCUSSION

Kinetic and Structural Background. Extensive studies by Benkovic and colleagues have led to the minimal kinetic pathway for the KF polymerase reaction (Scheme 1), and this serves as the framework for interpreting our experiments.

In the reaction of wild-type KF with correctly paired substrates, the chemical step of phosphoryl transfer is rapid and is bracketed by slower noncovalent steps (*15*). Experiments, such as rapid-quench measurements, which depend on the direct observation of covalent extension of the DNA primer strand, report the net effect of all steps of the reaction up to and including phosphoryl transfer (step 4 of Scheme 1). Because the noncovalent step 3 is slow, it determines the observed rate of correct nucleotide incorporation and is the step for which it is easiest to obtain information. The use of fluorescently labeled substrates, as in the present study, expands the capabilities of the kinetic analysis, allowing direct observation of some noncovalent steps and revealing steps that might not have been apparent from kinetic measurements of product formation.

Two strategies have been particularly helpful in this study. The use of both deoxy- and dideoxy-terminated primers allows the separation of steps preceding and following phosphoryl transfer. Additionally, use of more than one position for the fluorescent reporter improves our ability to detect noncovalent processes, since some positions may be more sensitive than others to particular conformational transitions. Data obtained with a variety of different DNA substrates should, nevertheless, be interpretable in a consistent manner, using a common reaction pathway with similar rates for the individual steps. A possible exception concerns experiments in which 2-AP is the templating base. Although 2-AP pairs with T in normal Watson−Crick geometry (*30*), polymerases such as KF can distinguish kinetically between A and 2-AP (this work and refs *35* and *42*). Our data show the efficiency of incorporation by KF of dTTP opposite 2-AP to be around 10-fold less than for a typical A-T base pair. Thus, although the 2-AP•dTTP pairing is a reasonable model for a correct nascent base pair, we expect to observe slightly less favorable kinetic parameters for reactions involving 2-AP at the 0 position, when compared with other reactions in which a normal A-T or G-C base pair is formed.

The available structures of KF homologues with substrates at the polymerase site may help to identify the physical processes responsible for the fluorescence changes reported by 2-AP at the 0 and +1 positions. Ternary complexes of polymerase, DNA, and the next complementary dNTP have been solved for T7 DNA pol, for *Bst* pol, and for a series of Klentaq complexes with all four nascent base pairs (*6*, *8*, *9*, *43*). These complexes appear poised for catalysis, which is prevented from taking place by the absence of a 3′-OH at the primer terminus. The structures, exemplified by one of the Klentaq complexes (Figure 8A), are very similar: the fingers subdomain is in the closed position, and the 0 position template base is stacked with the −1 template base and base paired with the incoming dNTP. Two metal ions are bound at the active site; metal B is coordinated to the dNTP phosphates, and metal A is in the correct position to coordinate a primer 3′-OH, though this hydroxyl group is absent in the dideoxy-terminated cocrystallization substrates. The +1 template base is dislocated by ≈180° from the template-primer duplex in all six ternary complex structures, but its exact position and interactions with the protein are not consistent.

The start point of our stopped-flow experiments could potentially be illustrated by polymerase−DNA binary complex structures, one of Klentaq (Figure 8B) and a series of

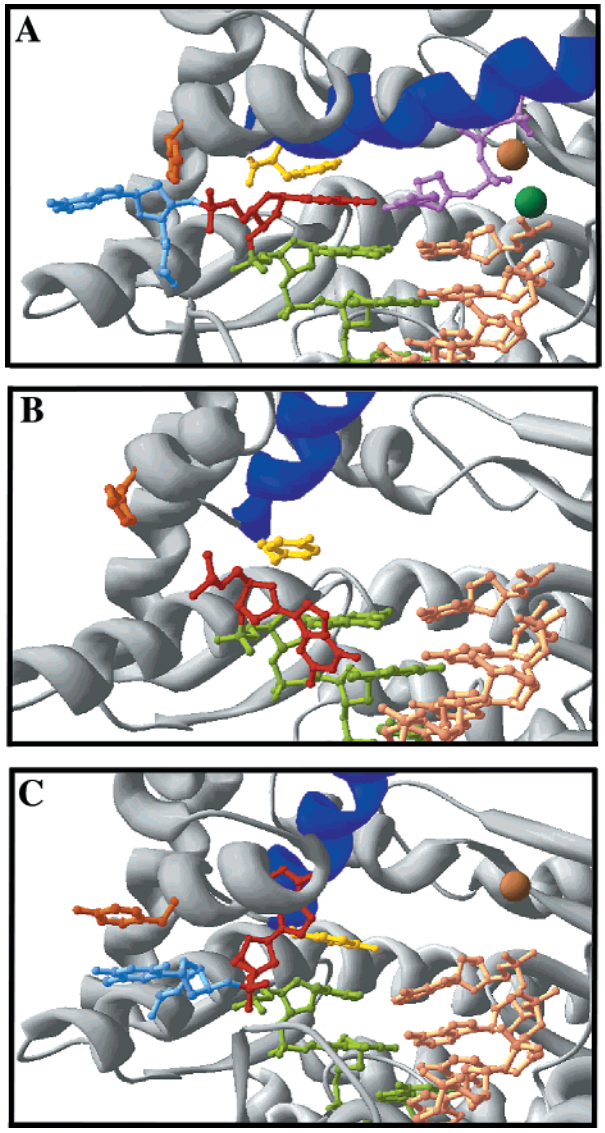

FIGURE 8: Comparison of the active site configuration in pol I family polymerase open and closed structures. The structures have been similarly oriented with respect to the primer-terminal base pair. In these figures, the template strand is shown in light green, except for the 0 and +1 positions which are shown in red and light blue, respectively. The primer strand is shown in beige, and the incoming nucleotide is in purple. The O helix is colored dark blue, and the residues equivalent to Y766 and F771 in KF (Y671 and H676 in Klentaq; Y714 and Y719 in *Bst* pol) are in yellow and orange, respectively. The Mg^{2+} ions in the metal A and metal B sites are shown in green and brown, respectively. As illustrated in this figure, the Klentaq ternary complex contains both metal A and metal B, the Klentaq binary complex has no metals in the active site, and the *Bst* pol binary complex has metal B only. Portions of the thumb subdomain have been removed so as not to obscure the active site residues. (A) Klentaq closed ternary complex (PDB entry 3KTQ, ref *6*). (B) Klentaq open binary complex (PDB entry 4KTQ, ref *6*). The +1 position base is not present in this structure because it was disordered. In this structure Y671 is partially stacked with the −1 base; however, in the related open ternary complex (PDB entry 2KTQ, ref *6*) the stacking interaction between Y671 and the −1 base is greater. (C) *Bst* pol open binary complex (PDB entry 4BDP, ref *7*). This figure was made using Swiss PDB Viewer (version 3.7b2) (*54*).

Bst pol cocrystals with DNA (e.g., Figure 8C) which show catalytic activity in the crystal (*6*, *7*). In some respects the Klentaq and *Bst* pol binary complex structures are similar: the fingers subdomain is in the open conformation, and the

0 position template base is unstacked from the template −1 base, which is itself stacked against the invariant Tyr at the C-terminal end of the O helix (Y671 of Klentaq or Y714 of *Bst* pol; the equivalent position in KF is Y766). However, there are significant differences in the position of the 0 position base in the two binary complex structures. The *Bst* pol structure shows the 0 position base in a pocket between the O and the O1 helices; the +1 base was visible in only one of the *Bst* pol cocrystal complexes and was stacked with Y719 (F771 in KF) on the surface of the fingers subdomain (*7*). By contrast, the Klentaq structure shows the 0 position base unstacked and folded back onto the template-primer duplex; the +1 base was disordered in this structure. Because the Klentaq binary complex was made by allowing the dNTP to diffuse out of a ternary complex, the structure may not represent a true binary complex, and this may account for the unusual position of the 0 position base. An intermediate complex of Klentaq, referred to as the "open ternary" complex, corresponds to removal of a fraction of the bound dNTP and has the same protein and DNA conformation as the binary complex described above, with the fingers subdomain in the open conformation. Additionally, a dNTP molecule is present at low occupancy in the same position seen in the ternary complex, stacked on the primer-terminal base pair, but with Y671 filling the place of the templating base. Metal B, associated with the dNTP phosphates, is present in the open ternary complex, but metal A is absent. The biological significance of the open ternary complex is unclear, but it may illustrate a species that could occur within the early steps of the reaction.

Early Steps in the Polymerase Reaction. Experiments in which correctly paired dNTPs are introduced opposite a templating base adjacent to 2-AP at the +1 position, or in which dTTP is paired opposite 2-AP at the 0 position, provide evidence for at least two fluorescently detectable steps before phosphoryl transfer. The earliest detectable step, observed when 2-AP is at the 0 position, is so rapid that its rate cannot be measured on the stopped-flow instrument, but the effect of this step can be seen as a change in the start point of the fluorescence signal (Figure 3A,B). Because it has the same dependence on dNTP concentration as does the rate of nucleotide incorporation, it is likely that this step corresponds to dNTP binding itself or to some conformational change that occurs very rapidly as a consequence of dNTP binding. The fluorescence decrease associated with this initial step indicates that it involves a change in the environment of the 0 position base such that the 2-AP fluorescence becomes more quenched. Assuming that the fluorescence of 2-AP primarily reports stacking interactions (*31*), the fluorescence decrease would be consistent with the structural changes associated with the transition from binary to ternary complex: specifically, movement of the 0 position base from a location where it is not stacked with the template-primer duplex to one where it is stacked with the −1 base and base paired with the incoming nucleotide.

The next step that is observable, when a correctly paired dNTP is added, produces an increase in the fluorescence of 2-AP at the template +1 position (Figure 5A,B). The fluorescence increase is very fast (around 500 s^{-1}) but, because it is detectable within the time scale of the stopped-flow instrument, it must occur after the step described above that produces the change in the start point of the 0 position experiment. The fluorescent reporter at the +1 position appears ideally located for detection of this second step. By contrast, the only fluorescence changes seen on a similar time scale with 2-AP at the 0 position were extremely small (Figure 3), indicating that this second step involves a change in environment that is essentially limited to the +1 position and is unlikely to be a large movement that affects most of the DNA in the active site. The observed fluorescence increase implies that addition of a correct dNTP to the binary complex changes the environment of the +1 base so that 2-AP fluorescence is less quenched; the rather limited information on the location of the +1 base in cocrystal structures does not indicate why this should be so. Our fluorescence emission data support the stacking interaction of the +1 base with the F771 side chain seen in the *Bst* pol binary complex structure but suggest that this interaction is largely unchanged in going from binary to ternary complex, because the F771A mutation increased the fluorescence of binary and ternary complexes to a similar extent.[3] The experiments with abasic sites were less conclusive but argue against any major contribution to the change in fluorescence of the +1 base due to stacking with the +2 base. Whatever the nature of this rapid second step, it seems likely that it has a counterpart in the reaction pathway of pol β since very similar fluorescence changes have been observed using a 2-AP reporter 5′ to the templating base (*32*).

When a normal deoxy-terminated primer is used, the rapid early fluorescence changes described above are followed by a fluorescence decay that is observable with the 2-AP reporter at either the 0 or +1 position. This fluorescence decay has a rate equal to that of nucleotide incorporation, as determined by rapid-quench experiments using the same substrates, and therefore reflects the rate of step 3, the rate-limiting step in the forward direction. This does not necessarily mean that the fluorescence change itself is a direct consequence of step 3; it may occur at step 3 and/or at a subsequent (more rapid) step. Because the fluorescence decrease associated with this third process is observed with 2-AP in both the 0 and +1 template positions, we infer that this process substantially alters the environment of both the 0 and the +1 bases and is therefore likely to be a more global change than the preceding step that affects only the +1 position. Given that the process of phosphoryl transfer (step 4) would not be expected to cause much movement of the substrates within the polymerase binding pocket, we suggest that the observed fluorescence signals may be caused by subsequent translocation of the 0 base to the −1 position and the +1 base to the 0 position.

Is the Closing of the Fingers an Early Step? As noted above, a 2-AP reporter at the 0 position undergoes a sizable and very rapid decrease in fluorescence associated with dNTP binding. The magnitude of the decrease is consistent with the dramatic change in the environment of the 0 position base that is seen when comparing binary and ternary complex structures, leading us to suggest that quenching of the 0 position 2-AP results from movement of the templating base into the active site pocket. Furthermore, we suggest that movement of the base is coupled to the conformational

[3] The recently published *Bst* pol ternary complex structure (*8*) does not clarify this issue because the relevant part of the structure is involved in a crystal contact.

changes of the protein that result in closing of the fingers subdomain because the open conformation has the side chain of Y766 (or its homologue) occupying the position that will be taken by the templating base. We do not expect that nucleotide binding alone, without the subsequent formation of the closed complex, would produce the large fluorescence decrease that we observe. Waksman and co-workers (*6*, *44*) have suggested two possible structures for the ternary complex that initially forms when a dNTP encounters the E·DNA binary complex: one would have the dNTP in contact with side chains of the O helix in the open conformation, and the other would have the dNTP positioned as in the open ternary complex, stacked on the primer terminus but with no templating base partner. Neither of these (admittedly hypothetical) structures results in a change in the environment of the templating (0 position) base; thus, to account for our observations, dNTP binding must be followed rapidly by further conformational transitions.

A key observation in support of the idea that the closed ternary complex forms immediately following dNTP binding is that the early rapid step is the only large amplitude fluorescence change seen when the primer strand is dideoxy terminated. Very similar results have been reported for T4 DNA polymerase and for pol β (*26*, *29*, *45*). The profound changes in the environment of the 0 position base that are apparent when comparing binary and ternary complex structures argue that formation of the closed complex would probably be associated with a substantial fluorescence change. Moreover, there is persuasive evidence for the formation of closed ternary complexes with dideoxy-terminated substrates, both in crystals (*6*, *9*, *43*) and in solution studies of KF, where addition of the cognate dNTP to a dideoxy-terminated E·DNA binary complex generates a more stable species (*38*, *46*, *47*).

If closing of the fingers subdomain is a rapid early step in the polymerase reaction, then one could question whether step 3 actually takes place with a dideoxy-terminated substrate or whether it is blocked by the absence of a primer 3′-OH, which serves as a ligand to the metal in site A. Close examination of the stopped-flow data obtained with a dideoxy primer and 2-AP at either the 0 or the +1 position (Figures 3B and 5B) shows an extremely low amplitude change whose rate is similar to that expected for step 3. We interpret these small changes cautiously as confirming that step 3 does indeed take place with the dideoxy-terminated substrate and that it is associated with a minimal change in fluorescence for either of the 2-AP reporters we have used. Consistent with this interpretation, the fluorescence signals obtained with dideoxy-terminated substrates were not augmented by attempts to increase occupancy of the metal A site by increasing the Mg^{2+} concentration or by using the tighter binding Mn^{2+}.

Consideration of the factors that affect the dNTP binding affinity provides a further argument that closing of the fingers subdomain is likely to be an early rapid step in the polymerase reaction pathway. In KF, dNTP binding is influenced both by the ability to form a correct base pair with the templating base and by the presence of important contact residues on the fingers subdomain (*16*, *17*, *48*). However, these two sets of contacts are mutually exclusive if the fingers are in the open conformation. To respond to both base pairing and the known side chain contacts requires the dNTP to experience the environment of the closed complex as part of the binding process, suggesting a rapid interconversion between open and closed ternary complexes. It seems very probable to us that the open and closed conformations may be in rapid equilibrium even in the uncomplexed and E·DNA forms of the enzyme, so that binding of a correctly paired dNTP would merely shift the equilibrium from predominantly open to predominantly closed. Observations with other polymerases are certainly consistent with the hypothesis that formation of the closed ternary complex occurs very early in the reaction pathway. Data from T4 DNA pol and pol β indicate that dNTP binding reflects interactions that require formation of the closed ternary complex (*27*, *49*). Moreover, for pol β, structural and fluorescence experiments using an exchange-inert dNTP−Cr(III) complex provide persuasive evidence linking formation of a closed complex to the very rapid fluorescence change that occurs early in the reaction (*28*, *29*).

The Identity of Step 3. If we are correct in our reasoning that the closing of the fingers subdomain is a rapid early step in the KF polymerase reaction pathway, then the question remains: what happens during the rate-limiting step 3? Our data suggest that this step does not produce significant fluorescence signals with either of the 2-AP reporter positions we have used and, therefore, that it may involve relatively subtle conformational rearrangements. Comparison of the open and closed ternary complexes shown in Figure 8 indicates two processes, in addition to the movement of the O helix and associated residues, that occur on forming the closed ternary complex. One is binding of the second divalent metal ion in site A, coordinated to the primer 3′-OH, and the second is rotation of the side chain of the active site carboxylate equivalent to D705 in KF. Moreover, the transitions associated with movement of the O helix need not necessarily take place as a single concerted step, so that other side chain motions could be proposed as candidates for step 3.

Although one should be cautious in drawing parallels between members of the polymerase superfamily and the unrelated pol β (*13*), suggestions similar to those listed above have been made concerning the step preceding phosphoryl transfer in pol β. On the basis of molecular dynamics simulations, Wilson and colleagues favor a rate-limiting rearrangement of critical active site side chains (*27*, *50*). Tsai and colleagues have proposed that step 3 corresponds to binding of the second metal ion in the site coordinated by the primer terminus (*29*) and have suggested that this step is rapid, so that there is no rate-limiting step before phosphoryl transfer (*24*). For pol β, the evidence for a rate-limiting noncovalent step relies solely on elemental effect data (*27*, *51*) and is certainly open to question. In the KF reaction pathway, however, there is convincing evidence for a slow step (step 3) preceding phosphoryl transfer, based on the nonequivalence of product yields from pulse−quench and pulse−chase experiments (*15*), and this is consistent with our observation of a slow, low-amplitude fluorescence change when the primer is dideoxy-terminated. We therefore interpret the experiments reported here from the standpoint that step 3 of the KF polymerase reaction pathway (Scheme 1) is indeed rate-limiting in the forward direction.

Incorporation of Incorrect Nucleotides. The conformational changes that occur during incorrect nucleotide incor-

poration show some significant differences from those that are observed during correct nucleotide addition. There was also considerable variation from mispair to mispair, hinting at interesting connections between mispair structure and reaction pathway. Because of this complexity, a full investigation of mispair formation was beyond the scope of the current study. However, one important conclusion that emerges from our data thus far is that the conformational changes around the +1 position during incorrect nucleotide incorporation are different from those that take place during correct nucleotide incorporation. None of the mispairs that we studied, using the +1 position 2-AP reporter, gave the rapid fluorescence increase (rate $\approx$500 s^{-1}) characteristic of correct dNTP addition. Thus, there appears to be a consistent position of the +1 base during correct nucleotide incorporation and alternative conformations of this base adopted during incorrect nucleotide incorporation, a conclusion that is supported by our $KMnO_4$ reactivity data.

KF Reaction Pathway: Implications for Fidelity. The results obtained in this study allow us to modify the minimal kinetic scheme for correct nucleotide incorporation derived from rapid-quench data. We propose that the E and E·DNA species are in rapid equilibrium between open and closed states and that binding of the correct dNTP (step 2) causes a shift in the equilibrium in favor of the closed conformation. A previously undetected step (step 2.1) that affects the environment of the +1 base takes place extremely rapidly after dNTP binding and formation of the closed ternary complex. Our data suggest the existence of other fairly rapid steps (2.2, 2.3, etc.) that are associated with only small changes in fluorescence. These early steps are followed by the rate-limiting noncovalent step (step 3) and then phosphoryl transfer. Our data suggest that step 3 takes place with a dideoxy-terminated primer and generates very little fluorescence signal with the 2-AP reporters we have used. As suggested for pol β, this step may involve binding of a second metal ion or movement of one or more active site side chains; its slow rate need not imply a dramatic conformational rearrangement.

Our preliminary results on misincorporation are intriguing in that they suggest that the pathways for correct and incorrect dNTP incorporations diverge, with structurally distinct species on the two pathways. The clearest example is step 2.1, which has a characteristic fluorescence signal (with a 2-AP reporter at the +1 position) that is only observed when a correct nucleotide is provided for incorporation. Polymerase fidelity has often been discussed in terms of induced fit (*19*, *52*): the ability of the correct substrate to induce conformational changes that result in the optimum positioning of active site residues. We believe the differences we see between correct and incorrect incorporations support this idea, particularly in the general formulation described by Post and Ray (*53*). According to the analysis by these authors, correct and incorrect dNTP substrates would induce different enzyme conformations in the ternary complex, consistent with the characteristic fluorescence signals mentioned above. Persistence of these substrate-dependent conformational differences into the transition state(s) would then generate specificity for the correct substrate. One could envisage a multistep pathway, such as the polymerase reaction, in two alternative, but equivalent ways: either a common pathway with different energetics and structures derived from correct and incorrect substrates, or two parallel but related pathways. Paradoxically, an induced fit enzyme with conformational flexibility of this type will have lower specificity for the correct substrate (i.e., fidelity) than a rigid enzyme whose active site is optimized for binding the correct substrate (*53*). Perhaps the conformational flexibility of polymerases represents a compromise between fidelity and other priorities, such as reaction rate, or the ability to negotiate modified or damaged template sites. Additionally, given that the active site of a polymerase needs to accommodate four favored substrate combinations (over twelve unfavored combinations), it may be difficult to provide this range of specificity within the context of a rigid enzyme.

ACKNOWLEDGMENT

We are grateful to Olga Potapova for excellent technical support, to Enrique M. De La Cruz for help and advice, and to Stephen J. Benkovic for comments on an earlier version of the manuscript.

SUPPORTING INFORMATION AVAILABLE

Examples of curve fitting and residuals for stopped-flow experiments using dP·0T1, dP·+1T1, and ddP·+1T1 substrates (Figures S1−S3). This material is available free of charge via the Internet at http://pubs.acs.org.

REFERENCES

1. Ollis, D. L., Brick, P., Hamlin, R., Xuong, N. G., and Steitz, T. A. (1985) Structure of large fragment of *Escherichia coli* DNA polymerase I complexed with dTMP, *Nature 313*, 762−766.
2. Steitz, T. A. (1999) DNA polymerases: structural diversity and common mechanisms, *J. Biol. Chem. 274*, 17395−17398.
3. Benkovic, S. J., and Cameron, C. E. (1995) Kinetic analysis of nucleotide incorporation and misincorporation by Klenow fragment of *Escherichia coli* DNA polymerase I, *Methods Enzymol. 262*, 257−269.
4. Joyce, C. M., and Steitz, T. A. (1994) Function and structure relationships in DNA polymerases, *Annu. Rev. Biochem. 63*, 777−822.
5. Brautigam, C. A., and Steitz, T. A. (1998) Structural and functional insights provided by crystal structures of DNA polymerases and their substrate complexes, *Curr. Opin. Struct. Biol. 8*, 54−63.
6. Li, Y., Korolev, S., and Waksman, G. (1998) Crystal structures of open and closed forms of binary and ternary complexes of *Thermus aquaticus* DNA polymerase I: structural basis for nucleotide incorporation, *EMBO J. 17*, 7514−7525.
7. Kiefer, J. R., Mao, C., Braman, J. C., and Beese, L. S. (1998) Visualizing DNA replication in a catalytically active *Bacillus* DNA polymerase crystal, *Nature 391*, 304−307.
8. Johnson, S. J., Taylor, J. S., and Beese, L. S. (2003) Processive DNA synthesis observed in a polymerase crystal suggests a mechanism for the prevention of frameshift mutations, *Proc. Natl. Acad. Sci. U.S.A. 100*, 3985−3900.
9. Doublié, S., Tabor, S., Long, A., Richardson, C. C., and Ellenberger, T. (1998) Crystal structure of a bacteriophage T7 DNA replication complex at 2.2 Å resolution, *Nature 391*, 251−258.
10. Franklin, M. C., Wang, J., and Steitz, T. A. (2001) Structure of the replicating complex of a pol α family DNA polymerase, *Cell 105*, 657−667.
11. Huang, H., Chopra, R., Verdine, G. L., and Harrison, S. C. (1998) Structure of a covalently trapped catalytic complex of HIV-1 reverse transcriptase: implications for drug resistance, *Science 282*, 1669−1675.
12. Sawaya, M. R., Prasad, R., Wilson, S. H., Kraut, J., and Pelletier, H. (1997) Crystal structures of human DNA polymerase β complexed with gapped and nicked DNA: evidence for an induced fit mechanism, *Biochemistry 36*, 11205−11215.
13. Holm, L., and Sander, C. (1995) DNA polymerase β belongs to an ancient nucleotidyltransferase superfamily, *Trends Biochem. Sci. 20*, 345−347.

14. Kuchta, R. D., Benkovic, P., and Benkovic, S. J. (1988) Kinetic mechanism whereby DNA polymerase I (Klenow) replicates DNA with high fidelity, *Biochemistry 27*, 6716−6725.
15. Dahlberg, M. E., and Benkovic, S. J. (1991) Kinetic mechanism of DNA polymerase I (Klenow fragment): identification of a second conformational change and evaluation of the internal equilibrium constant, *Biochemistry 30*, 4835−4843.
16. Eger, B. T., and Benkovic, S. J. (1992) Minimal kinetic mechanism for misincorporation by DNA polymerase I (Klenow fragment), *Biochemistry 31*, 9227−9236.
17. Carroll, S. S., Cowart, M., and Benkovic, S. J. (1991) A mutant of DNA polymerase I (Klenow fragment) with reduced fidelity, *Biochemistry 30*, 804−813.
18. Minnick, D. T., Liu, L., Grindley, N. D. F., Kunkel, T. A., and Joyce, C. M. (2002) Discrimination against purine-pyrimidine mispairs in the polymerase active site of DNA polymerase I: a structural explanation, *Proc. Natl. Acad. Sci. U.S.A. 99*, 1194−1199.
19. Wong, I., Patel, S. S., and Johnson, K. A. (1991) An induced-fit kinetic mechanism for DNA replication fidelity: direct measurement by single-turnover kinetics, *Biochemistry 30*, 526−537.
20. Kuchta, R. D., Mizrahi, V., Benkovic, P. A., Johnson, K. A., and Benkovic, S. J. (1987) Kinetic mechanism of DNA polymerase I (Klenow), *Biochemistry 26*, 8410−8417.
21. Herschlag, D., Piccirilli, J. A., and Cech, T. R. (1991) Ribozyme-catalyzed and nonenzymatic reactions of phosphate diesters: rate effects upon substitution of sulfur for a nonbridging phosphoryl oxygen atom, *Biochemistry 30*, 4844−4854.
22. Polesky, A. H., Dahlberg, M. E., Benkovic, S. J., Grindley, N. D. F., and Joyce, C. M. (1992) Side chains involved in catalysis of the polymerase reaction of DNA polymerase I from *Escherichia coli*, *J. Biol. Chem. 267*, 8417−8428.
23. Capson, T. L., Peliska, J. A., Kaboord, B. F., Frey, M. W., Lively, C., Dahlberg, M., and Benkovic, S. J. (1992) Kinetic characterization of the polymerase and exonuclease activities of the gene 43 protein of bacteriophage T4, *Biochemistry 31*, 10984−10994.
24. Showalter, A. K., and Tsai, M.-D. (2002) A reexamination of the nucleotide incorporation fidelity of DNA polymerases, *Biochemistry 41*, 10571−10576.
25. Doublié, S., Sawaya, M. R., and Ellenberger, T. (1999) An open and closed case for all polymerases, *Struct. Folding Des. 7*, R31−35.
26. Shah, A. M., Li, S.-X., Anderson, K. S., and Sweasy, J. B. (2001) Y265H mutator mutant of DNA polymerase β. Proper geometric alignment is critical for fidelity, *J. Biol. Chem. 276*, 10824−10831.
27. Vande Berg, B. J., Beard, W. A., and Wilson, S. H. (2001) DNA structure and aspartate 276 influence nucleotide binding to human DNA polymerase β. Implication for the identity of the rate-limiting conformational change, *J. Biol. Chem. 276*, 3408−3416.
28. Zhong, X., Patel, S. S., and Tsai, M.-D. (1998) DNA polymerase β. Dissecting the functional roles of the two metal ions with Cr(III)dTTP, *J. Am. Chem. Soc. 120*, 235−236.
29. Arndt, J. W., Gong, W., Zhong, X., Showalter, A. K., Liu, J., Dunlap, C. A., Lin, Z., Paxson, C., Tsai, M.-D., and Chan, M. K. (2001) Insight into the catalytic mechanism of DNA polymerase β: structures of intermediate complexes, *Biochemistry 40*, 5368−5375.
30. Sowers, L. C., Fazakerley, G. V., Eritja, R., Kaplan, B. E., and Goodman, M. F. (1986) Base pairing and mutagenesis: observation of a protonated base pair between 2-aminopurine and cytosine in an oligonucleotide by proton NMR, *Proc. Natl. Acad. Sci. U.S.A. 83*, 5434−5438.
31. Rachofsky, E. L., Osman, R., and Ross, J. B. A. (2001) Probing structure and dynamics of DNA with 2-aminopurine: effects of local environment on fluorescence, *Biochemistry 40*, 946−956.
32. Dunlap, C. A., and Tsai, M.-D. (2002) Use of 2-aminopurine and tryptophan fluorescence as probes in kinetic analyses of DNA polymerase β, *Biochemistry 41*, 11226−11235.
33. Jia, Y., Kumar, A., and Patel, S. S. (1996) Equilibrium and stopped-flow kinetic studies of interaction between T7 RNA polymerase and its promoters measured by protein and 2-aminopurine fluorescence changes, *J. Biol. Chem. 271*, 30451−30458.
34. Mandal, S. S., Fidalgo da Silva, E., and Reha-Krantz, L. J. (2002) Using 2-aminopurine fluorescence to detect base unstacking in the template strand during nucleotide incorporation by the bacteriophage T4 DNA polymerase, *Biochemistry 41*, 4399−4406.
35. Frey, M. W., Sowers, L. C., Millar, D. P., and Benkovic, S. J. (1995) The nucleotide analog 2-aminopurine as a spectroscopic probe of nucleotide incorporation by the Klenow fragment of *Escherichia coli* polymerase I and bacteriophage T4 DNA polymerase, *Biochemistry 34*, 9185−9192.
36. Derbyshire, V., Freemont, P. S., Sanderson, M. R., Beese, L., Friedman, J. M., Joyce, C. M., and Steitz, T. A. (1988) Genetic and crystallographic studies of the 3′,5′-exonucleolytic site of DNA polymerase I, *Science 240*, 199−201.
37. Joyce, C. M., and Derbyshire, V. (1995) Purification of *E. coli* DNA polymerase I and Klenow fragment, *Methods Enzymol. 262*, 3−13.
38. Turner, R. M., Jr., Grindley, N. D. F., and Joyce, C. M. (2003) Interaction of DNA polymerase I (Klenow fragment) with the single stranded template beyond the site of synthesis, *Biochemistry 42*, 2373−2385.
39. Astatke, M., Grindley, N. D. F., and Joyce, C. M. (1998) How *E. coli* DNA polymerase I (Klenow fragment) distinguishes between deoxy- and dideoxynucleotides, *J. Mol. Biol. 278*, 147−165.
40. Sambrook, J., Fritsch, E. F., and Maniatis, T. (1989) *Molecular Cloning*: *A Laboratory Manual*, 2nd ed., Cold Spring Harbor Laboratory, Cold Spring Harbor, NY.
41. Smith, R. M., Martell, A. E., and Chen, Y. (1991) Critical Evaluation of Stability Constants for Nucleotide Complexes with Protons and Metal Ions, *Pure Appl. Chem. 63*, 1015−1080.
42. Bloom, L. B., Otto, M. R., Beechem, J. M., and Goodman, M. F. (1993) Influence of 5′-nearest neighbors on the insertion kinetics of the fluorescent nucleotide analogue 2-aminopurine by Klenow fragment, *Biochemistry 32*, 11247−11258.
43. Li, Y., and Waksman, G. (2001) Crystal structures of a ddATP-, ddTTP-, ddCTP-, and ddGTP-trapped ternary complex of Klen-taq1: insights into nucleotide incorporation and selectivity, *Protein Sci. 10*, 1225−1233.
44. Li, Y., Kong, Y., Korolev, S., and Waksman, G. (1998) Crystal structures of the Klenow fragment of *Thermus aquaticus* DNA polymerase I complexed with deoxyribonucleoside triphosphates, *Protein Sci. 7*, 1116−1123.
45. Fidalgo da Silva, E., Mandal, S. S., and Reha-Krantz, L. J. (2002) Using 2-aminopurine fluorescence to measure incorporation of incorrect nucleotides by wild type and mutant bacteriophage T4 DNA polymerases, *J. Biol. Chem. 277*, 40640−40649.
46. Dzantiev, L., Alekseyev, Y. O., Morales, J. C., Kool, E. T., and Romano, L. J. (2001) Significance of nucleobase shape complementarity and hydrogen bonding in the formation and stability of the closed polymerase-DNA complex, *Biochemistry 40*, 3215−3221.
47. Dzantiev, L., and Romano, L. J. (2000) A conformational change in *E. coli* DNA polymerase I (Klenow fragment) is induced in the presence of a dNTP complementary to the template base in the active site, *Biochemistry 39*, 356−361.
48. Astatke, M., Grindley, N. D. F., and Joyce, C. M. (1995) Deoxynucleoside triphosphate and pyrophosphate binding sites in the catalytically competent ternary complex for the polymerase reaction catalyzed by DNA polymerase I (Klenow fragment), *J. Biol. Chem. 270*, 1945−1954.
49. Yang, G., Franklin, M., Li, J., Lin, T. C., and Konigsberg, W. (2002) Correlation of the kinetics of finger domain mutants in RB69 DNA polymerase with its structure, *Biochemistry 41*, 2526−2534.
50. Yang, L., Beard, W. A., Wilson, S. H., Broyde, S., and Schlick, T. (2002) Polymerase β simulations suggest that Arg258 rotation is a slow step rather than large subdomain motions per se, *J. Mol. Biol. 317*, 651−671.
51. Werneburg, B. G., Ahn, J., Zhong, X., Hondal, R. J., Kraynov, V. S., and Tsai, M.-D. (1996) DNA polymerase β: pre-steady-state kinetic analysis and roles of arginine-283 in catalysis and fidelity, *Biochemistry 35*, 7041−7050.
52. Johnson, K. A. (1993) Conformational coupling in DNA polymerase fidelity, *Annu. Rev. Biochem. 62*, 685−713.
53. Post, C. B., and Ray, W. J., Jr. (1995) Reexamination of induced fit as a determinant of substrate specificity in enzymatic reactions, *Biochemistry 34*, 15881−15885.
54. Guex, N., and Peitsch, M. C. (1997) SWISS-MODEL and the Swiss-Pdb Viewer: an environment for comparative protein modeling, *Electrophoresis 18*, 2714−2723.

BI0341206